Chemistry and Physics of Lipids 218 (2019) 47–56

Contents lists available at ScienceDirect

Chemistry and Physics of Lipids

journal homepage: www.elsevier.com/locate/chemphyslip

PEG-grafted phospholipids in vesicles: Effect of PEG chain length and concentration on mechanical properties

Amit Mahendra, Honey Priya James, Sameer Jadhav*

Department of Chemical Engineering, Indian Institute of Technology Bombay, Powai, Mumbai 400076, India

ARTICLE INFO

Keywords:
Biomembrane
Giant unilamellar vesicle
Liposome
Vesicle-micelle transition
Bending rigidity

ABSTRACT

Incorporation of low molecular weight poly-ethylene glycol (PEG) - grafted phospholipids in vesicle bilayers is known to increase the circulation time of liposomal drug delivery vehicles. Mechanical properties of giant unilamellar DPPC vesicles containing varying concentrations of DSPE-PEG (PEG MW: 550, 1000 and 2000) were measured by micropipette aspiration assay or osmotic swelling. While the area compressibility modulus did not change significantly, the bending modulus and water permeability of the bilayer was found to increase with increasing mole fraction of DSPE-PEG. This increase was more pronounced for higher molecular weight PEG. The measured bending modulus agreed with that predicted by scaling theory only at low mole fractions of DSPE-PEG. The water permeability was also measured as a function of the increase in area per lipid (due to steric repulsion between PEG chains), and for the same area per lipid, the PEG chain with MW 550 provided a greater resistance to water transport across the vesicle membrane compared to PEG 1000 and 2000. Lysis tension of the membrane, determined by osmotic lysis method at different loading rates showed a decrease in membrane strength on inclusion of the polymer lipid. These results suggest that liposome lifetime in the circulation and the rate of drug delivery are affected by the molecular weight and concentration of PEG in the bilayer.

1. Introduction

Liposomes are spherical capsules formed by self-assembly of phospholipids into bilayers that not only encapsulate but are also suspended, in the aqueous medium. Liposomes are increasingly used for targeted delivery and controlled release of both hydrophilic and hydrophobic drugs (Allen and Cullis, 2013; Gabizon et al., 1997; Lasic, 1998). DPPC has been used widely because of its application in drug delivery, especially in thermosensitive liposomes. The major characteristic of thermosensitive liposomes is the retention of the drug at room temperature as well as normal body temperature of 37 ^{0}C while releasing it at slightly higher temperatures. Therefore, DPPC, which has a phase transition temperature of 41^{0}C, is popularly used for liposomal drug delivery (Hossann et al., 2014).

One of the major issues faced with liposomal drug delivery was the rapid clearance of liposomes from the circulatory system by the reticuloendothelial system (RES) (Allen and Cullis, 2013; Devine et al., 1994). In the last few decades, several methods have been adopted to modify the surface properties of liposomes for improving their circulation half-life (Gabizon et al., 1990; Gabizon and Papahadjopoulos, 1988). Polyethylene glycol (PEG) is an inert, hydrophilic, nonionic, flexible polymer chain, which provides a steric barrier and increased hydrophilicity to the liposomal surface (Pasut and Veronese, 2012; Woodle, 1995). Therefore, liposomes with PEG-grafted phospholipids are not easily recognized by the immune system and have shown greater stability with prolonged circulations times in the host compared to non-PEGylated liposomes (Allen and Hansen, 1991; Blume and Cevc, 1990; Klibanov et al., 1990; Lasic, 1997; Needham and Rudoll, 1993; Pasut and Veronese, 2012; Woodle et al., 1994).

Many studies have demonstrated a significant increase in the blood circulation half-life, low RES uptake, and increased membrane permeability of PEGylated liposomes (stealth liposomes), properties which are governed by molecular weight and concentration of the grafted PEG present in the bilayer (Allen and Hansen, 1991; Parr et al., 1994). Results from *in vivo* pharmacokinetic studies (Dos Santos et al., 2007) showed that the inclusion of lower molecular weight DSPE - PEGs (PEG MW: 350, 550, 750 and 2000) show significantly longer blood circulation time compared to pure DSPC liposomes. However, liposomes with high molecular weight DSPE-PEGs (PEG MW: 5000 and 12,000) were found to be unstable and showed reduced concentrations in the blood compared to low molecular weight DSPE PEGs (PEG MW: 1000 and 2000) (Maruyama et al., 1992). It has been shown that in addition to long circulation half-life, membrane permeability, encapsulation efficiency and the ability of liposome to retain the encapsulated drug for

* Corresponding author.
E-mail address: srjadhav@iitb.ac.in (S. Jadhav).

https://doi.org/10.1016/j.chemphyslip.2018.12.001
Received 5 July 2018; Received in revised form 10 November 2018; Accepted 1 December 2018
Available online 03 December 2018
0009-3084/

transport to the target site, play an important role in the efficacy of liposomal drug delivery systems (Lasic, 1997). Increasing the mole fraction of higher molecular weight PEG in the bilayer is known to reduce the encapsulation efficiency for water soluble drugs (Maruyama et al., 1992). This has been attributed to a larger volume fraction of the vesicle core being occupied by the longer PEG chains arranged on the inner leaflet of the vesicle as well as to the increase in the fraction of micelles coexisting with the vesicles. Studies have also shown that the increased membrane permeability with increasing mole fraction of higher molecular weight PEG lipid makes such liposomes unsuitable for drug delivery due to the leakage of encapsulated cargoes (Edwards and Almgren, 1992; Hashizaki et al., 2005; Nicholas et al., 2000).

To date, several experimental studies have focused on physicochemical properties, phase transition, encapsulation efficiency and vesicle-to-micelle transition of PEGylated liposomes (Lasic and Needham, 1995; Nicholas et al., 2000; Sriwongsitanont and Ueno, 2002). Moreover, there have been quite a number of theoretical predictions focused on the mechanical properties of lipid bilayers grafted with polymer lipids (Marsh, 2001; Marsh et al., 2003; Needham et al., 1992). According to DeGennes (DeGennes, 1979), at lower surface concentration of a grafted polymer, the polymer chains do not interact with each other leading to a randomly coiled “mushroom” conformation whereas, at higher polymer concentrations, the steric repulsion between neighboring polymer chains results in an extended “brush” configuration. These lateral interactions between polymer chains leads to a significant increase in the bending modulus (Marsh et al., 2003).The scaling theory of polymer brushes predicts that the stiffness of a bilayer membrane increases with polymer chain length and grafting density in the brush regime (Alexander, 1977; DeGennes, 1979). Evans and coworkers (Evans and Rawicz, 1997) carried out micropipette aspiration of giant unilamellar vesicles to study the concentration dependent variation on area compressibility and bending moduli of vesicles containing high molecular weight DSPE-PEG (PEG MW: 2000, 5000 and 12000). However, even though low molecular weight PEG liposomes have been widely used as drug delivery systems, to the best of the authors’ knowledge, there are no estimates of their mechanical properties. In the present study, we investigated the effects of low molecular weight DSPE-PEG (PEG MW: 550, 1000 and 2000) on vesicle properties such as lysis tension, water permeability as well as area compressibility and bending moduli of PEG-grafted DPPC liposomes. Moreover, we also estimated the actual PEGylated to pure lipid ratio in the bilayer as a function of the composition used to prepare the vesicles, since these are known to differ due to vesicle-to-micelle transition. Furthermore, we compared our results to the theoretical predictions of bending modulus by scaling theory. These results provide a better understanding of the effect of PEGylated lipids on mechanical properties of liposomes and may bear significant implications for the development of stealth liposomal drug delivery systems.

2. Materials and methods

2.1. Materials

1,2-distearoyl-*sn*-glycero-3-phosphoethanolamine-N-[methoxy (polyethylene glycol)-550] (DSPE-PEG 550), 1,2-distearoyl-*sn*-glycero-3- phosphoethanolamine-N-[methoxy(polyethylene glycol)-1000] (DSPE-PEG 1000), 1,2-distearoyl-*sn*-glycero-3- phosphoethanolamine-N-[amino (polyethylene glycol)-2000] (DSPE-PEG 2000), and 1,2-dipalmitoyl-*sn*-glycero-3- phosphocholine (DPPC) in chloroform solutions were purchased from Avanti Polar Lipids Inc (Alabaster, AL, USA). Indium tin oxide (ITO) coated glass slide of dimension (25 mm × 75 mm × 1.1 mm) were procured from Delta Technologies (Stillwater, MN, USA). Ethanol, chloroform and other solvents were from Merck (Mumbai, India), while bovine serum albumin (fraction V, low heavy metals), sucrose and glucose were from Himedia (Mumbai, India). Nuclepore track- etched polycarbonate membrane of pore radius 200 nm were procured from Whatman Inc. (Clifton, NJ, USA). Polydimethylsiloxane (PDMS, Sylgard 184) was purchased from Dow Corning (Michigan, USA). All solutions were prepared using deionized water with a resistivity of 18 MΩ-cm from a Merck-Millipore system (Mumbai, India).

2.2. Fabrication of micropipettes

Micropipettes were prepared from standard borosilicate glass capillaries having outer and inner diameters 1.00 mm and 0.58 mm, respectively (Narishige, Japan). The capillaries were pulled using a micropipette puller (PC-10, Narishige, Japan) such that the central region reduced in diameter where it eventually splits into two sections. The tip of each section was then fractured, bent and fire polished using a microforge (MFG-5, Microdata Instruments Inc, Germany) to obtain micropipettes having an inner diameter between 8 to 10 µm. The micropipettes were then coated with 0.02% w/v aqueous BSA solution. The coated pipettes were washed extensively with distilled water and 0.1 M glucose solution to ensure that excess BSA on the pipette was removed.

2.3. Preparation of giant unilamellar vesicles

Giant unilamellar vesicles were obtained by the electroformation method (Estes and Mayer, 2005). Briefly, stock solutions of DPPC were diluted to 2 mg/ml in a mixed solvent of 2:1 volumetric ratio of chloroform to methanol. 50 µl of lipid in chloroform solution (2 mg/ml) was spin-coated (PRK-6k, Photoresist spinner, Ducom Instruments, Bangalore, India) on the conductive surfaces of two ITO-coated glass slides. The slides were then placed in desiccators under vacuum for a minimum of two hours to ensure complete evaporation of chloroform. The two slides were placed with their conductive sides facing each other and separated by a 2 mm thick PDMS frame to form a chamber that was sealed with silicon grease. The dried lipid film was then gently hydrated using 0.1 M sucrose solution that had been preheated to 60 ^{0}C such that hydration occurred above the phase transition temperature of DPPC (41 ^{0}C). The chamber was then placed in an oven at 60 ^{0}C. An alternating current (AC) field with an amplitude of 3 V (peak-to-peak) and frequency of 10 Hz was then applied to the ITO slides using a function generator (33220 A, Agilent Technologies, CA, USA). The temperature of the chamber was carefully monitored throughout the electroformation process to make sure it did not fall below 50 ^{0}C and after two hours, GUVs of size ranging from 10 to 40 µm were formed. The chamber was slowly cooled to room temperature (24 ^{0}C) and the vesicle suspension was collected and stored at 4 ^{0}C in 2 ml polypropylene microcentrifuge tubes. Vesicles containing PEGylated DSPE (PEG MW: 550, 1000 and 2000) and DPPC were prepared by the previously described electroformation method at various DSPE-PEG/DPPC molar ratios. These GUVs were used for experiments within 2 days of preparation. The vesicles were extruded through nuclepore track-etched polycarbonate membranes (Diameter: 25 mm) having pore radius of 200 nm for vesicle-to-micelle transition studies (Patil et al., 2012).

2.4. Micropipette aspiration measurement

A custom-made micropipette aspiration chamber (1 cm × 1 cm × 6 mm) was made by placing U-shaped silicone rubber spacer on a bottom coverslip and then placing another cover slip on the top of the spacer. The coverslips used for making the micropipette aspiration chamber were passivated with 0.2% w/v BSA solution to prevent adhesion of GUVs to the glass. The aspiration chamber was placed inside a Plexiglas housing on the microscope stage of an inverted microscope (Eclipse TE 2000-U, Nikon, Japan) equipped with a 40x long-working distance differential interference contrast (DIC) objective. A high resolution, cooled, charge-coupled device (CCD) camera (RETIGA-2000R, Q Imaging, Canada) was used for capturing the images. The vesicles

were mixed with equi-osmolar solution of glucose to create refractive index contrast between the inside and outside of the vesicle that facilitated the optical detection of vesicle projection length inside the micropipette.

The temperature of the Plexiglas housing, mounted on the microscope stage, was controlled using a microcontroller with a digital display, connected to an electric heating element and a temperature sensor which were placed inside the housing. The temperature could be set between 25 ^{0}C to 50 ^{0}C with an accuracy of 0.5 ^{0}C. The vesicles containing (100 mM sucrose) were mixed with glucose solution (100 mM) and kept for equilibration at the desired temperature (43 ^{0}C) for 20 min inside the Plexiglas housing. A small drop of the vesicle suspension (100 µl) was carefully placed into the micropipette aspiration chamber with a micropipette such that it was held between the upper and lower glass coverslips due to surface tension thereby avoiding contact with the silicone rubber sidewalls. Thus the sample did not get contaminated with silicone grease.

To control its movement, the micropipette was connected to a micromanipulator (MHW-3, Narishige, Japan) and was filled with the same solution (0.1 M glucose) as found in the chamber. To control the suction pressure, the micropipette was connected to a water reservoir mounted on a mechanical slider through a thin water-filled silicone tube. The vertical position of the reservoir was first adjusted to match the height of the pipette and water reservoir so that no flow was observed at the pipette tip. The vertical displacement (lowering) of the reservoir relative to the chamber resulted in a negative suction pressure. The temperature was maintained at 43 ^{0}C during all experiments.

Unilamellar vesicles with a diameter between 25–40 µm were chosen for all experiments. Individual vesicles were aspirated with a glass micropipette (Fig. 1A), and the applied suction pressure ΔP was related to the induced isotropic membrane tension τ using Young-Laplace equation (Evans and Needham, 1987)

$$\tau = \frac{\Delta P R_p}{2\left(1 - \frac{R_P}{R_v}\right)} \quad (1)$$

Where, R_P and R_V represent the radii of the pipette and vesicle, respectively. The increase in length ΔL_p of the part of vesicle sucked into the micropipette (Fig. 1A, B) was measured as a function of the applied negative pressure. If A_0 represents the vesicle surface area measured at an initial low tension state and A is the area after application of tension, the observed or apparent area strain is given by $\alpha = (A - A_0)/A_0$. The apparent area strain is related to the change in projection length, ΔL_p, by (Evans and Needham, 1987; Evans and Rawicz, 1990)

$$\alpha = \frac{2\pi R_p \Delta L_p}{A_0}\left(1 - \frac{R_p}{R_v}\right) \quad (2)$$

The area strain of an aspirated vesicle may be related to the bending and area compressibility moduli by the following expression (Evans and Rawicz, 1990)

$$\alpha = \left(\frac{k_B T}{8\pi k_c}\right) ln\left(1 + \frac{c_0 \tau A}{k_c}\right) + \frac{\tau}{K_A} \quad (3)$$

Where k_B, T, k_c and K_A represent the Boltzmann constant, absolute temperature, bending modulus and direct area compressibility modulus, respectively. $c_0 \sim 0.1$, is a constant dependent on modes used to represent surface undulations (Rawicz et al., 2000). In Eq. (3), the first term represents the increase in membrane area due to smoothening out of membrane undulations while the second term accounts for membrane area increase due to direct stretching of the membrane. The bending modulus is calculated by multiplying the slope of $ln(\tau)$ vs. α_{app} plot (Fig. 1C) in the low tension range (< 0.5 mN/m) with $k_B T/8\pi$ (Evans and Rawicz, 1990). The slope of the τ vs. α_{app} plot (Fig. 1D) in the high tension regime (> 0.5 mN/m) gives the apparent area compressibility modulus, K_{app} (Rawicz et al., 2000). The direct area strain, α_{dir}, was obtained by subtracting the logarithmic contribution from α_{app} and the slope of the τ vs. α_{dir} gave the direct area compressibility modulus, K_{dir} (Fig. 1D). The appropriate contribution to be subtracted is given by $\Delta\alpha(i)$, for each $(i)th$ value of α_{app} (Ly and Longo, 2004)

$$\Delta\alpha(i) = \left(\frac{k_B T}{8\pi k_{c(avg)}}\right) ln\left(\frac{\tau(i)}{\tau(1)}\right) \quad (4)$$

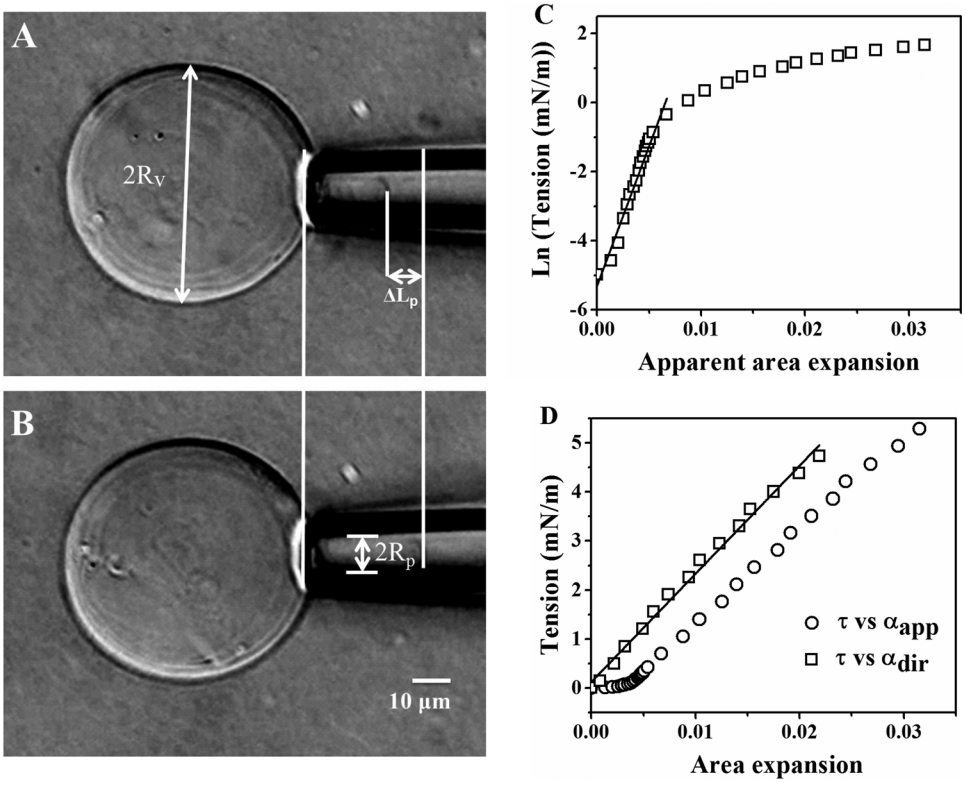

Fig. 1. Tension and area strain of a vesicle measured by micropipette aspiration. Pure DPPC giant unilamellar vesicle, in fluid phase at 43 ^{0}C, were aspirated into a micropipette. Tension was estimated from applied suction pressure using Eq. (1). Area strain was estimated from measurements of original radius of vesicle, radius of aspirated vesicle and projected length of the vesicle section in the micropipette using Eq. (2). DIC images of the vesicle held by micropipette at low tension (0.5 mN/m), (A) and at high tension (4.5 mN/m), (B). (C) Slopes of the plot of natural logarithm of tension vs apparent area strain in the region of low tension regime (< 0.5 mN/m) yields bending modulus for bilayer. The mean bending modulus (k_c) for DPPC vesicles in the fluid phase was found to be 0.9×10^{-19} J. (D) Slope of the tension vs apparent area strain in the high tension regime yields apparent area compressibility modulus (186 mN/m). The direct area compressibility modulus was obtained by removing the contributions from smoothing of thermal undulations using Eqs. (3) and (4) and the mean value for direct area compressibility modulus was found to be 220 mN/m.

Where $k_{C(avg)}$ is the average bending modulus and $\tau(1)$ represents the initial low tension state.

Based on scaling theory, bending modulus and area per lipid for a bilayer membrane containing polymer grafted lipids were estimated to be, respectively, (Hristova and Needham, 1994), (Marsh et al., 2003),

$$k_c^p = k_B T a_m^{\left(2mf+\frac{10}{3}\right)} n_p^3 \left(\frac{x_p}{A_1}\right)^{\left(mf+\frac{5}{3}\right)} \tag{5}$$

and

$$A_1^2 = A_{1,0}^2 + m_f \frac{k_B T}{\gamma} a_m^{2mf} n_p x_p^{mf+1} A_1^{1-mf} \tag{6}$$

Where $A_{1,0} \sim 0.7\,nm^2$ is area per lipid molecule of DPPC in the fluid phase, $m_f = \frac{5}{6}$ is an exponent showing dependency of polymer free energy on grafting density (Marsh et al., 2003), $\gamma = 3.9 \times 10^{-20} J\,nm^{-2}$ is the hydrophobic free energy density (Marsh, 1996), n_p is the degree of polymerisation, X_P is mole fraction of polymer grafted lipid in the bilayer and $a_m = 0.39\,nm$ is the size of monomer unit.

In all experiments, we checked the reversible behavior of each vesicle before aspirating for the entire range of tension (0.01 to 5 mN/m) for measurements. To this end, pre-stressing of vesicles was carried out by aspirating them into the micropipette upto a membrane tension of 0.1 mN/m and then releasing them. By this procedure, we could confirm whether the vesicles stuck to the glass and these were omitted (< 20 percent of the total population). After pre-stressing, the same vesicle was aspirated for the entire range of tension to measure the bending and area compressibility moduli. To this end, vesicles were initially held at a suction pressure corresponding to a very low membrane tension (~ 0.01 mN/m). The suction pressure was then increased in a stepwise manner with 5 s waiting period to allow the system to equilibrate after each step. We aspirated vesicles from 0.01 to 0.5 mN/m to determine their bending moduli and > 0.5 mN/m to measure the area compressibility moduli. The radii of the micropipette and vesicle as well as the length of vesicle aspirated into the micropipette were estimated at each instant, using Image *J* software (imagej.nih.gov).

2.5. Measurement of water permeability across lipid bilayer

To measure water permeability of the lipid bilayer, a vesicle was selected and transferred using a micropipette from a chamber containing 0.1 M glucose solution (iso-osmolar with respect to sucrose solution inside the vesicle) to an adjacent chamber containing a hypertonic (0.11 M) glucose solution. To transfer the vesicle, it was held by a micropipette at a tension of ~0.5 mN/m and inserted into a transfer pipette that was filled with 0.1 M glucose solution and mounted on another manipulator. The micropipette holding the vesicle and the transfer pipette enveloping the vesicle were then lifted to the middle height of the chamber containing 0.1 M glucose solution. The microscope manipulation stage was moved laterally so that vesicle and tips of both the pipettes were translocated to the chamber containing the 0.11 M glucose solution. The two pipettes and the vesicle were then lowered into this chamber and the transferring pipette was removed without disturbing the vesicle. The above-mentioned procedure helps avoid exposing the vesicle to the small air gap between the chambers. The temperature of the setup was maintained at 43 °C. The vesicle exposed to the hypertonic glucose solution and a strong osmotic force ($> 10^5$ Pa) which drew water out of the vesicle. The volume change of the vesicle was measured as a function of time. Throughout the test, the vesicle was held under a fixed suction pressure to control bilayer tension ~0.5 mN/m. The volume change of vesicle, ΔV, was estimated from the change in the projection length of the vesicle inside micropipette, ΔL_p, as follows (Olbrich et al., 2000)

$$\Delta V = V - V_0 = -\pi R_p (R_v - R_p) \Delta L_p \tag{7}$$

Where V and V_0 are the volume of the GUV at time $t = t$ and $t = 0$ respectively. The rate of change of vesicle volume per unit surface area is determined by (Olbrich et al., 2000)

$$\frac{1}{A}\left(\frac{dV}{dt}\right) = -(P_f V_w)\Delta C \tag{8}$$

Where '*A*' is the area of the GUV, P_f is the water permeability coefficent of the bilayer, V_w is the molar volume of water and ΔC is the difference in osmolarity across the bilayer. By normalising the instantaneous volume with the final volume $\left(V^* = \frac{V}{V_\infty}\right)$, the time dependent change in vesicle volume is given by

$$\frac{dV^*}{dt} = -k\left(\frac{V^* - 1}{V^*}\right) \tag{9}$$

Where $k = P_f C_\alpha^{in} v_w \left(\frac{A}{V_\infty}\right)$ and C_α^{in} represents the final concentration inside the vesicle. To determine the value of P_f a nonlinear fitting algorithm is employed to match Eq. (9) to the time-dependent change in volume of each vesicle tested (Olbrich et al., 2000).

2.6. Estimation of onset and completion of transition from vesicle to micelle phase

Previous theoretical and experimental studies have shown that when concentration of polymer-lipid in the vesicle exceeds a threshold value, the bilayer becomes unstable leading to formation of micellar phase coexisting with the vesicular phase. The onset of micelle formation X_P^{ON} was estimated from the theoretical expression $X_P^{ON} \sim n_p^{\frac{-1}{mf+1}}$ given by (Marsh et al., 2003). The end point of the vesicle to micelle transition, X_P^{END} for DSPE-PEG 550, 1000 and 2000 were obtained from dynamic light scattering (Zetasizer, Nano ZS, Malvern Instruments, UK) measurements of the suspensions containing vesicles and/or micelles. The total fraction of lipid (both pure and polymer-grafted) present in vesicle phase is given by (Marsh et al., 2003),

$$f_{tot(V)} = 1 - \left(\frac{X_P - X_P^{ON}}{X_P^{END} - X_P^{ON}}\right) \tag{10}$$

Where, X_P is total mole fraction of polymer lipid (both in vesicular and micellar phase). The fraction of polymer lipid in the vesicle phase $f_{p(V)}$ is given by,

$$f_{p(V)} = 1 - \frac{X_P^{end}}{X_P} f_{tot(V)} \tag{11}$$

The actual mole fraction of polymer-lipid in vesicle is given by,

$$X_P^V = \frac{f_{p(V)} X_P}{f_{tot(V)}} \tag{12}$$

For DPPC: DPSE-PEG 550, the size measurements were carried out for several concentration such as 10, 20, 25, 30, 40, 60 and 80 mol % to observe (i) the coexistence of vesicle and micelle and (ii) micelle only. Similar measurements were done at 5, 10, 15, 20, 30, 40 and 60 mol % for DSPE-PEG 1000 and 5, 10, 15, 20 and 40 mol % for DSPE-PEG 2000 (not all data shown). We also obtained DLS measurements of pure DPPC vesicles for comparison.

2.7. Electron microscopy of DPPC vesicles

Liposome samples were imaged in a cryogenic mode (Quorum PP3000 T) using scanning electron microscopy (JSM 7600 F, JEOL, MA, USA). To this end, a small drop of liposome suspension was placed onto the sample holder and frozen by plunging into liquid nitrogen (-190 ^{0}C). The frozen sample was then transferred into the SEM chamber and subjected to sublimation for 5 min. Further, the images were captured at voltage 5.0 kV and magnification of 12,000 X and the size distribution analysis was carried out using Image *J* software (imagej.nih.gov).

2.8. Determination of lysis tension of the vesicle

To measure the lysis tension of vesicles, a single vesicle containing sucrose solution is selected and transferred by a micropipette to an adjacent chamber containing Milli-Q water. After the transfer, the microscopic images of vesicles were recorded until they ruptured. The osmotic pressure difference across the bilayer causes water to permeate into the vesicle. The resulting increase in the volume of the vesicle causes an increase in tension of the bilayer membrane and leads to its eventual rupture. The rate of increase in vesicle diameter with time was used to measure its surface area and rate of fractional area change was multiplied by area compressibility modulus to obtain the loading rate ($d\tau/dt$). The rate of increase in membrane tension (loading rate) may be assumed to be time - invariant provided the vesicle volume as well as difference in osmolarity across the vesicle bilayer does not change substantially. The lysis tension of the vesicle was calculated by

$$\tau_{lys} = K_A \frac{\Delta A}{A_o} \tag{13}$$

Where ΔA is difference in area prior to rupture and the initial area is A_0. Vesicles were formed in 0.1 M, 0.5 M, and 5 M sucrose solutions prior to their transfer to Milli-Q water, thereby subjecting them to three different loading rates. The lysis tension experiments were conducted at 43 °C.

3. Results and discussion

Giant vesicles of pure DPPC as well as those with a mixture of PEG-grafted DSPE and DPPC were prepared. The molecular weight of the grafted PEG as well as DSPE-PEG: DPPC ratio in lipid mixture was varied and the physical properties of the vesicles such as area compressibility modulus, bending modulus, water permeability and lysis tension were measured.

3.1. Effect of PEG molecular weight and ratio of DSPE-PEG to DPPC on bending modulus and area compressibility modulus

The bending modulus and area compressibility modulus of pure DPPC vesicles as well as those containing a mixture of DSPE-PEG and DPPC were measured at 43 ^{0}C (ensuring bilayer exists in liquid crystalline phase) using micropipette aspiration method. The logarithm of tension plotted as a function of the apparent area strain (Fig. 2A) showed a difference between pure DPPC vesicles and DPPC vesicles containing 0.2 mol fraction DSPE-PEG in the low area strain regime (below 0.01). This low area strain regime was used to estimate the bending modulus using Eq. (3) (Evans and Rawicz, 1990) and was plotted as a function of mole fraction of PEGylated lipid (MW: PEG: 550, 1000 and 2000) in the mixture of DSPE-PEG and DPPC used to prepare the giant vesicles. The bending modulus was found to increase and eventually saturate with increasing mole fraction of grafted DSPE-PEG (Fig. 2B). Moreover, for vesicles prepared with longer PEG chain length, the increase in bending modulus was more pronounced and the saturation values were relatively higher when compared to low mol. wt. PEG vesicles (Fig. 2B). Our results show trends similar to a previous micropipette aspiration study (Evans and Rawicz, 1997) where it was observed that the bending modulus of fluid-phase digalactosyl diacylglycerol (DGDG) increased upon addition of DSPE-PEG of various molecular weights (PEG MW: 2000, 5000 and 12000). The increase in bending modulus has been attributed to repulsion between PEG chains and has been predicted theoretically using scaling theory by Eq. (5) (Hristova and Needham, 1994). The predicted increase in bending modulus shows good agreement with our experimental results at lower mole fractions of DSPE-PEG but fails to match the saturation observed at a higher DSPE-PEG concentration in the vesicles (Fig. 2B). The saturation in bending modulus value at large PEG-lipid mole fractions has been attributed to a transition to micelle phase as the vesicle phase is unable to hold the high concentration of PEG-lipid (Marsh et al., 2003) which is discussed later.

Next, we investigated the effect of increasing concentration of polymer grafted lipid on vesicle area expansion modulus. To this end, the membrane tension was plotted as a function of direct area strain (Fig. 2C), which is estimated by correcting the measured area strain (apparent area strain) for contribution from membrane bending (Rawicz et al., 2000). We observed that area compressibility modulus of vesicles composed of DSPE-PEG and DPPC mixture did not show significant variation from that measure for pure DPPC vesicles for all concentrations and molecular weights of grafted PEG used in this study (Fig. 2D). Our area expansion modulus data is in agreement with observations of (Evans and Rawicz, 1997) with DGDG vesicles containing DSPE-PEG.

3.2. Effect of PEG molecular weight and ratio of DSPE-PEG to DPPC on water permeability across the lipid bilayer

Subsequently, we studied the effect of polymer lipid on the permeability of vesicles to water. To this end, we transferred a GUV using a micropipette at a small fixed pressure to a hypertonic glucose solution which resulted in a decrease in vesicle volume due to water removal from vesicle to the exterior until the system reached equilibrium. The decrease in vesicle volume was measured by the increase in projection length inside the micropipette at a fixed aspiration pressure (Fig. 3A). The percent change in vesicle volume was plotted as a function of time and the water permeability of the vesicle with and without PEG was estimated by fitting Eq. (9) to the experimental data (Fig. 3B). We made several such measurements on single GUVs (n = 10) and the obtained average value of water permeability for DPPC membrane was 12.95 ± 1.16 μm/s at 43 ^{0}C. When transferred to the hypertonic glucose solution, DPPC vesicles with grafted DSPE-PEG took less time to achieve equilibrium than the DPPC vesicles at the same temperature of 43 ^{0}C. The effect of different molecular weight and concentration of PEG lipids on the permeability of water through vesicles is shown in (Fig. 3C). The results indicate that incorporation of PEG-grafted lipids increases the permeability of water across the bilayer.

The increased water permeability of PEG grafted vesicles may be explained in terms of area expansion of lipid membranes caused by the inclusion of PEG lipid. Steric interactions between grafted polymers give rise to a lateral pressure, which tends to expand the membrane. This lateral pressure induced area expansion was verified experimentally by the increase in motional freedom of spin-labeled lipid chains on incorporating polymer-grafted lipids in bilayer membranes, as reported by (Montesano et al., 2001). By assuming lipid chain volume is conserved in fluid membranes, the increased area per molecule can be related to decrease in the membrane thickness. The increase in area per lipid molecule accompanied with decrease in membrane thickness implies that the lipid membrane becomes more disordered or loosely packed with high degree of gauche conformation. This increase in membrane fluidity with the addition of polymer lipid was experimentally demonstrated in a previous study (Pantusa et al., 2003). The lateral diffusion coefficient of DOPC in supported lipid bilayers after treating with 30% wt/wt aqueous solution of PEG(MW: 8000) showed a dramatic increase to 51.4 ± 2.6 $\mu m^2 s^{-1}$ as compared to 7.9 ± 0.2 $\mu m^2 s^{-1}$ for pure DOPC in supported lipid bilayers (Tabarin et al., 2012). Furthermore, our data is in agreement with earlier work showing that increase in membrane permeability in the presence of micelle forming polymer lipids (DSPE-PEG 2000) at a concentration greater than 20 mol percent (Edwards et al., 1997; Edwards and Almgren, 1992).

3.3. Vesicle-to-micelle transition

In an aqueous dispersion, while pure phospholipids form bilayers, polymer grafted lipids such as DSPE-PEG have a tendency to form micelles due to enlargement of the hydrophilic head groups. In mixtures of

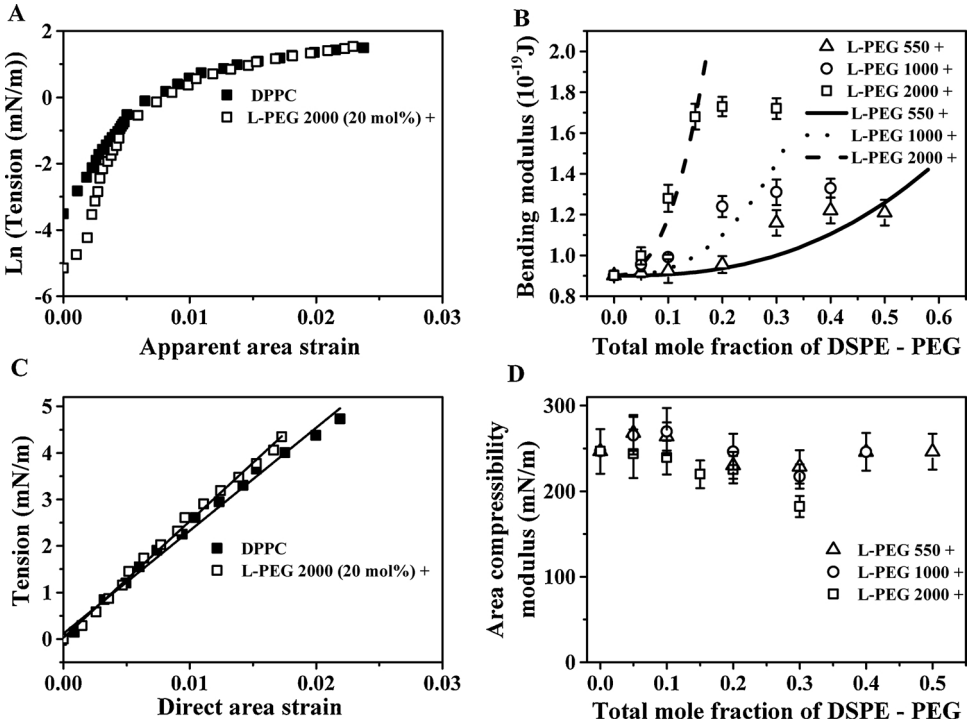

Fig. 2. Effect of molecular weight of PEG and DSPE-PEG mole fraction on bending and area compressibility moduli of DPPC/DSPE-PEG vesicles. (A) Plots of $ln(\tau)$ vs. area strain (α) for DPPC vesicles with and without 20 mol percent DSPE-PEG 2000 show differences in low tension but not high tension regimes. (B) Bending modulus (k_c) of DPPC/DSPE-PEG bilayers as a function of mole fraction of DSPE-PEG (PEG MW 550, 1000, 2000). The lines are predictions of scaling theory (Marsh et al., 2003). (C) Tension vs direct area strain plots of DPPC vesicles with and without 20 mol percent DSPE-PEG 2000. (D) Direct area expansion modulus of DPPC/DSPE-PEG vesicles measured as a function of mole fractions of DSPE-PEG (PEG MW: 550, 1000, 2000). Measurements for a minimum of eight vesicles at each composition were plotted as mean ± std. dev.

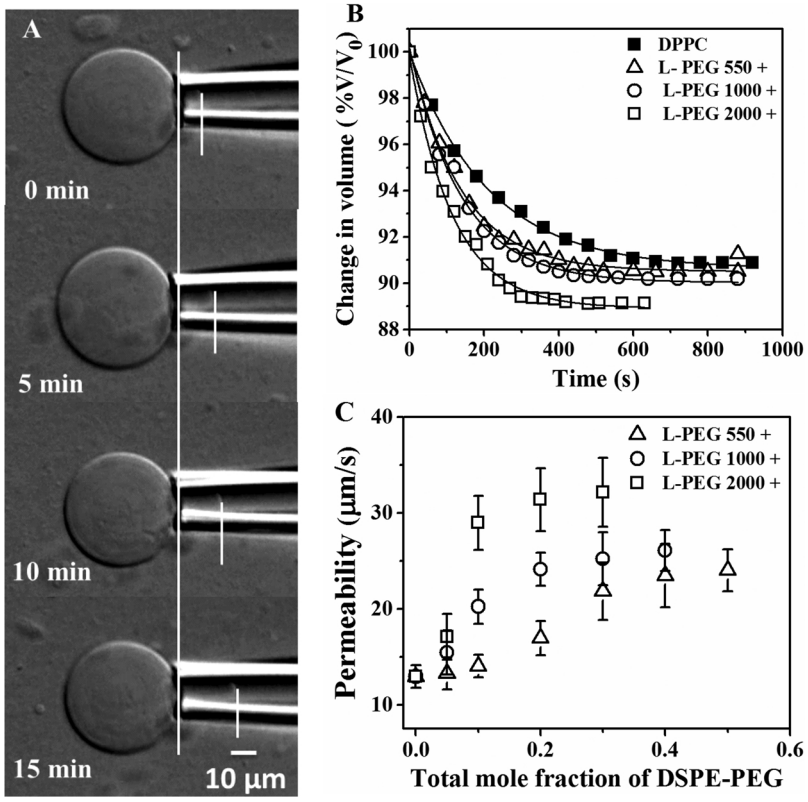

Fig. 3. Effect of molecular weight of PEG and DSPE-PEG mole fraction on water permeability of DPPC/DSPE-PEG vesicles. (A) DIC images of DPPC vesicle held by micropipette when GUV is exposed to hypertonic solutions of glucose. The increase in aspiration length inside the micropipette (shown by vertical white line) indicates a reduction in vesicle volume when the GUV is transferred from 0.1 M glucose to 0.11 M glucose (43 ^{0}C). (B) Volume change of vesicle obtained after the transfer of GUV to the hypertonic glucose solution. The mole ratio used for vesicles composed of DPPC/DSPE-PEG is 90:10. (C) Permeability of DPPC/DSPE-PEG vesicles as a function of total mole fraction of DSPE-PEG (PEG MW: 550, 1000, 2000). Values represented as mean ± std. dev. (n ≥ 10).

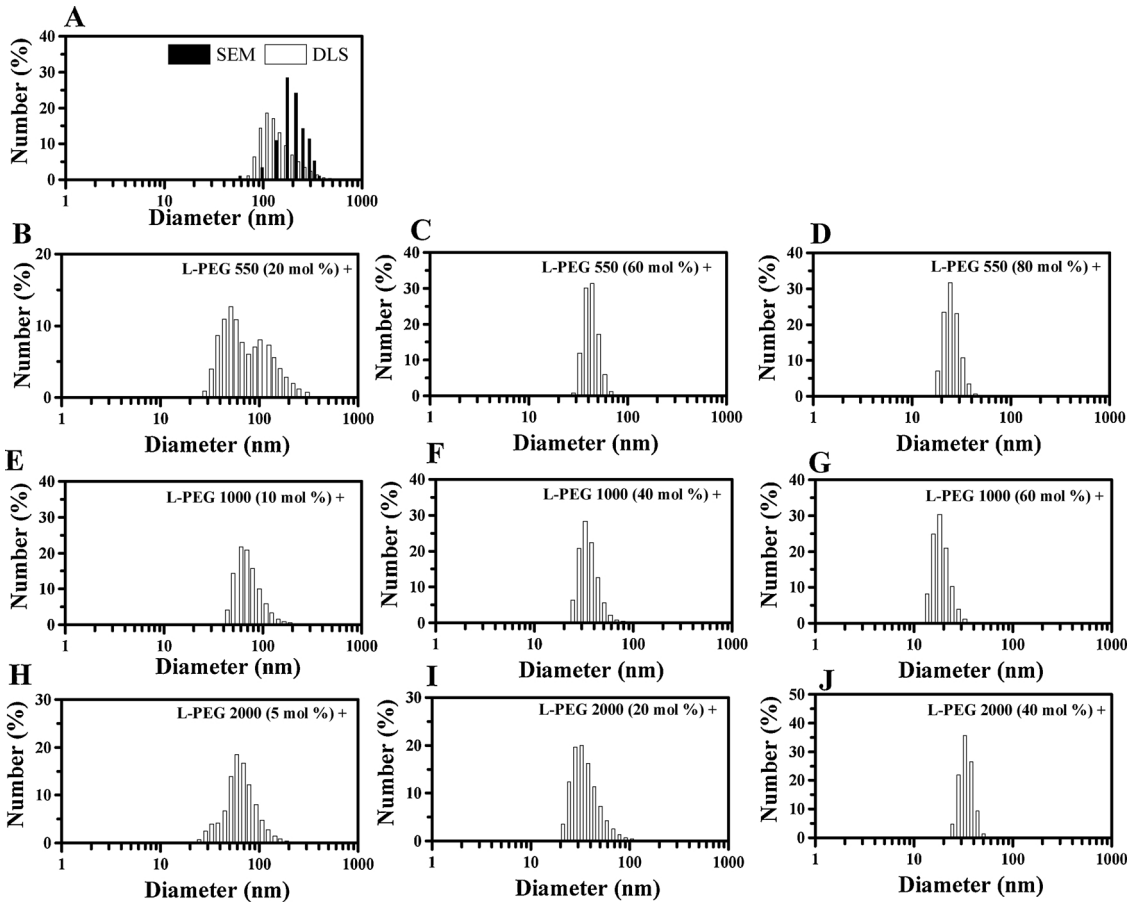

Fig. 4. Vesicle-to-micelle transition of DPPC/DSPE-PEG vesicles. (A) Liposome size distribution of pure DPPC suspensions obtained by DLS and SEM. Coexistence of vesicles and micellar phase was observed for (B) 20 mol percent DSPE-PEG 550, (E) 10 mol percent DSPE-PEG 1000, and (H) 5 mol percent DSPE-PEG 2000. Higher micelle to vesicle ratio was observed for (C) 60 mol percent DSPE-PEG 550, (F) 40 mol percent DSPE-PEG 1000, and (I) 20 mol percent DSPE-PEG 2000. Pure micellar phase was observed for (D) 80 mol percent DSPE-PEG 550, (G) 60 mol percent DSPE-PEG 1000, and (*J*) 40 mol percent DSPE-PEG 2000.

pure and polymer grafted lipids, both vesicles and micelles may coexist, with the fraction of micelles increasing with increasing concentration of polymer grafted lipids (Belsito et al., 2000; Marsh et al., 2003). The transition from a suspension of only vesicles to a mixture of vesicles and micelles and finally to a dispersion containing only micelles is a function of the fraction of polymer grafted lipid as well as the molecular weight of the grafted polymer, and has been investigated by several groups (Edwards et al., 1997; Johnsson et al., 2001; Montesano et al., 2001; Sandstrom et al., 2007). Moreover, for a given molecular weight of grafted polymer, it has been reported that the fraction of polymer grafted lipid present in micelle and bilayer (vesicle) phase differ and are functions of the total polymer grafted lipid to pure lipid ratio in the dispersion (Garbuzenko et al., 2005). Thus the polymer lipids can be incorporated in the bilayer forming lipid up to a certain saturation concentration without forming micelles. Estimates of X_P^{ON} from Eq. (10) for DSPE-PEG and DPPC system for PEG molecular weights of 550, 1000 and 2000, were found to be 0.26, 0.18 and 0.12 respectively.

X_P^{END} values for our system were obtained from dynamic light scattering data to capture transition from suspensions having both vesicles and micelles to pure micellar suspensions for various mixtures of DPPC with DSPE-PEG having PEG molecular weights of 550, 1000 and 2000 (Fig. 4). We first obtained the size distribution of pure DPPC vesicles (mean diameter 196 nm) and compared the same to that obtained from cryo-SEM, where the mean diameter was 213 nm (Fig.4 Panel A). The small difference may be attributed to statistical sampling errors for small sample sizes of cryo-SEM data. Next we ascertained, whether mixed vesicular and micellar phase were observed for DSPE-PEG suspensions. The micellar and vesicular populations are clear in case of DPPC: DSPE-PEG 550 (Fig. 4, Panel B), while the ratio of vesicle to micelle is smaller in the case of DPPC: DSPE-PEG 1000 and DPPC: DSPE-PEG 2000 to observe two peaks (Fig. 4, Panel E and H). Further increase in DSPE-PEG concentration led to an increase in the micelle-to-vesicle ratio. Specifically, panels C (60 mol percent DSPE-PEG 550), F (40 mol percent DSPE-PEG 1000) and I (20 mol percent DSPE-PEG 2000) of (Fig. 4) show a largely micellar suspension with the presence of a small fraction of vesicles having size greater than 50 nm. Increasing the DSPE-PEG concentration resulted in pure micellar suspensions indicated by absence of particles having size greater than 50 nm as observed from panels D (80 mol percent DSPE-PEG 550), G (60 mol percent DSPE-PEG 1000) and *J* (40 mol percent DSPE-PEG 2000) of (Fig. 4). Therefore, X_P^{END} values were taken as 0.8, 0.6 and 0.4 for PEG molecular weights of 550, 1000 and 2000 respectively.

The amount of polymer lipid in the vesicle phase was calculated using Eq. (12) and the actual mole fraction of polymer lipid in vesicles was plotted as a function of mole fraction of polymer lipid in mixture (Fig. 5A). Next, we plotted the bending modulus and water permeability of the bilayer membranes as a function of the actual composition of the vesicle bilayer. The bending modulus was found to increase with increase in mole fraction of PEG-lipid in the vesicle (Fig. 5B), though it did not obey the predictions of Eq. (5) based on scaling theory (DeGennes, 1979; Hristova and Needham, 1994; Marsh et al., 2003). The permeability of lipid bilayer was plotted as a function of actual mole fraction of polymer lipid in vesicle phase for the different molecular weights of PEG (Fig. 5C). The area of the bilayer per lipid molecule was calculated using Eq. (6) for the various polymer-lipid mixtures and the water permeability across vesicle was plotted as a function of

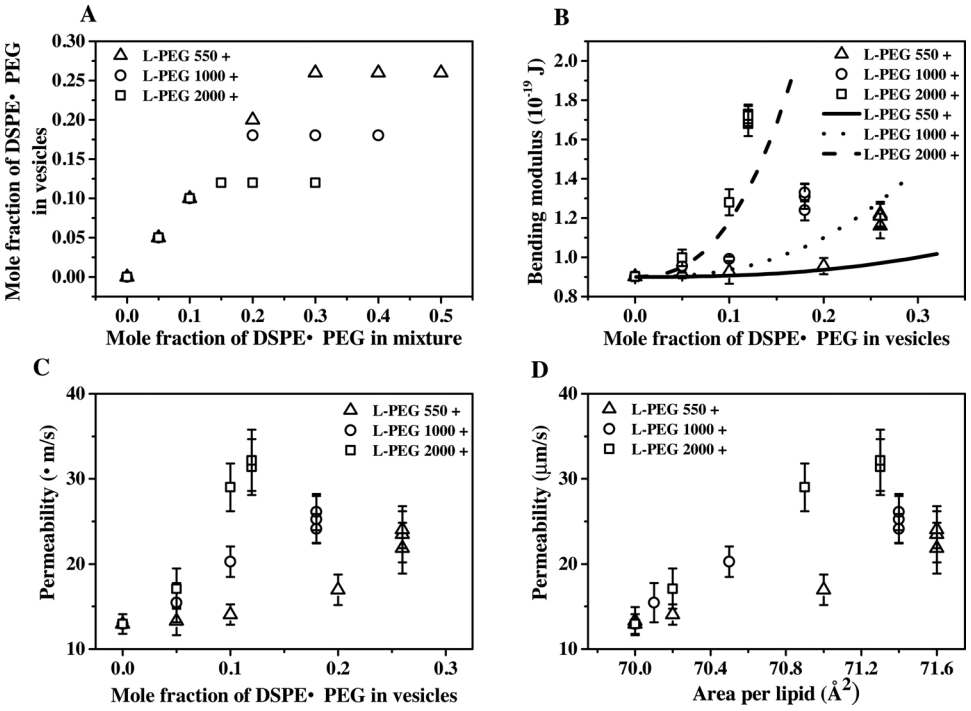

Fig. 5. Mechanical properties of the bilayer as a function of actual mole fraction of DSPE-PEG in vesicles. (A) The actual mole fraction of DSPE-PEG in vesicle vs. total mole fraction of DSPE-PEG in the system (mixture). (B) The bending modulus of the bilayer as a function of mole fraction of DSPE-PEG (PEG MW 550, 1000, 2000) in the vesicles. (C) Water permeability of the bilayer as a function of mole fraction of DSPE-PEG (PEG MW: 550, 1000, 2000) in the vesicles. (D) Water permeability plotted as a function of area per lipid of DPPC/ DSPE-PEG bilayer (PEG MW: 550, 1000, 2000).

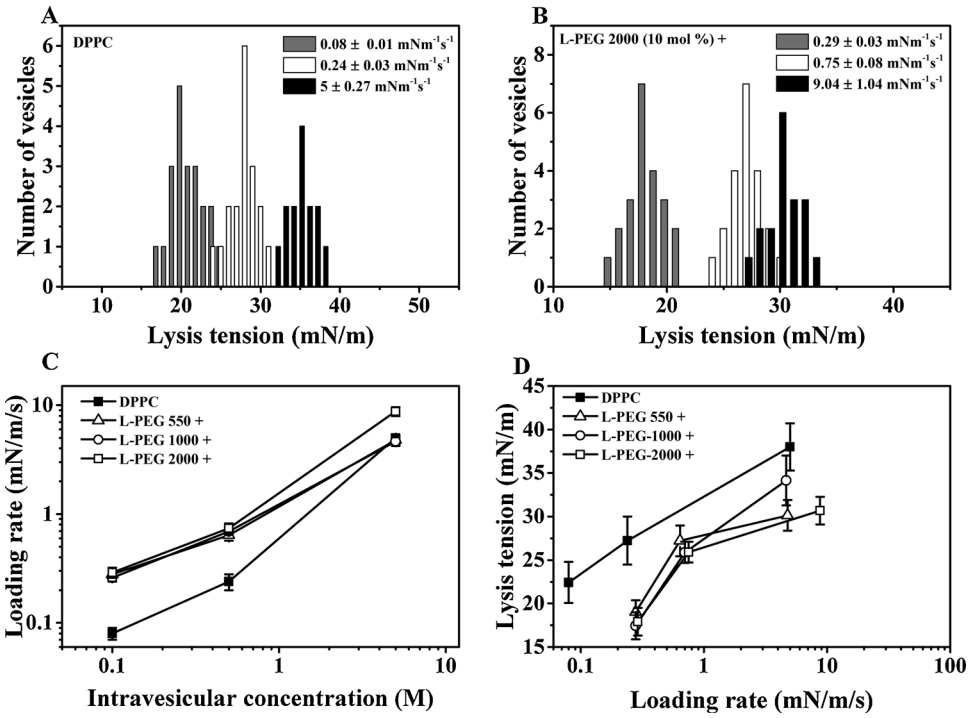

Fig. 6. Lysis tension of DPPC and DPPC/DSPE-PEG vesicles at different loading rates estimated by osmotic lysis method. (A) Distribution of lysis tension values for varying loading rates measured at 43 ^{0}C for pure DPPC (A) and DPPC/ DSPE-PEG 2000 vesicles (B). (C) Effect of intra-vesicular sucrose concentration on the loading rates for DPPC and DPPC/DSPE-PEG vesicles. (D) Lysis tension as a function of loading rate for pure DPPC and DPPC/DSPE-PEG vesicles. The DPPC: DSPE-PEG mole ratio was 90:10. Data represented as mean ± std. dev.

area per lipid (Fig. 5D). We observe that the presence of the grafted PEG: (i) causes an increase in area per lipid and hence permeability of the bilayer and, (ii) provides additional resistance to water transport through the lipid bilayer sandwiched between grafted polymer layers. The resistance to water permeability across the vesicle membrane due to the layers of grafted PEG decreases with increasing molecular weight of the polymer (Fig. 5D).

3.4. Effect of PEG molecular weight and ratio of DSPE - PEG to DPPC on vesicle lysis tension-

The mechanical strength of vesicle membrane was measured using the osmotic lysis method. We estimated the lysis tension of vesicles for three loading rates corresponding to vesicles formed in 0.1 M, 0.5 M, and 5 M sucrose. Since vesicle rupture is a stochastic process, we plotted the distribution of lysis tensions for the vesicles of a particular composition at a given loading rate. Histograms of lysis tension at different loading rate for vesicles made from pure DPPC and DPPC: DSPE - PEG 2000 (90:10) at 43 ^{0}C are shown in (Fig. 6A, B). The mean positions of

the histograms shift towards the right with an increase in the loading rate, which implies increase in lysis tension with higher loading rate. This is in agreement with previous work by Evans and coworkers (Evans et al., 2003) who showed that vesicles rupture at larger values of tensions when subjected to faster rates of loading. The dependence of loading rate on different intravesicular sucrose concentration for vesicles composed of pure DPPC with and without PEG grafted lipid is shown in (Fig. 6C). The higher water permeability of DSPE - PEG vesicles containing sucrose solution of a particular concentration results in a larger loading rate when compared to that of pure DPPC vesicles. Our data show that the addition of PEG-lipids leads to a decrease in lysis tension of vesicles. The reduction in lysis tension was more prominent at lower loading rates (Fig. 6D). The decrease in the lysis tension of PEG grafted lipid may also be explained on the basis of mean field and scaling theory available for polymer brushes (Hristova and Needham, 1994). The lateral repulsion between the grafted polymer brushes opposes the attractive hydrophobic interaction between lipid chains resulting in a lower lysis tension for vesicles containing polymer-grafted lipids. A decrease in membrane edge tension leading to membrane thinning and a concomitant reduction lysis tension has also been previously reported in other vesicle systems (Karatekin et al., 2003; Portet and Dimova, 2010).

4. Conclusion

In this study, micropipette aspiration was used to investigate the effect of polymer-grafted lipids on the mechanical properties and permeability of giant vesicles. Our data show that bending stiffness and permeability of giant vesicles increase with increasing concentration of the polymer grafted lipids in the bilayer and the increase is more pronounced for longer polymer chains. The presence of polymer grafted lipids does not show significant change in the area compressibility modulus. Also, the presence of polymer-grafted lipids in vesicle bilayers resulted in lower mean lysis tension values. Taken together, while a higher concentration of polymer-grafted lipid in the bilayer results in steric stabilization of the vesicle to deformation, it also leads to an increased bilayer permeability and the tendency for vesicle rupture. These results may have significant implications in designing liposomal drug delivery systems as one may have to account for a significant increase in the leakage of encapsulated cargoes from PEGylated liposomes. Our study underlines the fact that fundamental insights into the behavior of vesicular systems are critical for the rational design of therapeutic strategies.

Conflict of interest

Authors declare no conflict of interest.

Acknowledgments

The authors are grateful to the IIT Bombay cryo-scanning electron microscopy facility. Authors acknowledge financial support from Department of Science and Technology (DST), (Government of India) through IRHPA scheme. HPJ was supported by DST Inspire Fellowship (DST/INSPIRE/03/2014/001092).

References

Alexander, S., 1977. Adsorption of chain molecules with a polar head a scaling description. J. Phys. 38, 983–987. https://doi.org/10.1051/jphys:01977003808098300.

Allen, T.M., Cullis, P.R., 2013. Liposomal drug delivery systems: from concept to clinical applications. Adv. Drug Deliv. Rev. 65, 36–48. https://doi.org/10.1016/j.addr.2012.09.037.

Allen, T.M., Hansen, C., 1991. Pharmacokinetics of stealth versus conventional liposomes: effect of dose. Biochim. Biophys. Acta 1068, 133–141. https://doi.org/10.1016/0005-2736(91)90201-I.

Belsito, S., Bartucci, R., Montesano, G., Marsh, D., Sportelli, L., 2000. Molecular and mesoscopic properties of hydrophilic polymer-grafted phospholipids mixed with phosphatidylcholine in aqueous dispersion: Interaction of dipalmitoyl N-poly(ethylene glycol)phosphatidylethanolamine with dipalmitoylphosphatidylcholine studied by spectrophotometry and spin- label electron spin resonance. Biophys. J. 78, 1420–1430. https://doi.org/10.1016/S0006-3495(00)76695-1.

Blume, G., Cevc, G., 1990. Liposomes for the sustained drug release in vivo. Biochim. Biophys. Acta 1029, 91–97. https://doi.org/10.1016/0005-2736(90)90440-Y.

DeGennes, P.G., 1979. Scaling Concepts in Polymer Physics. Cornell university press.

Devine, D.V., Wong, K., Serrano, K., Chonn, A., Cullis, P.R., 1994. Liposome—complement interactions in rat serum: implications for liposome survival studies. Biochim. Biophys. Acta 1191, 43–51. https://doi.org/10.1016/0005-2736(94)90231-3.

Dos Santos, N., Allen, C., Doppen, A.M., Anantha, M., Cox, K.A.K., Gallagher, R.C., Karlsson, G., Edwards, K., Kenner, G., Samuels, L., Webb, M.S., Bally, M.B., 2007. Influence of poly(ethylene glycol) grafting density and polymer length on liposomes: Relating plasma circulation lifetimes to protein binding. Biochim. Biophys. Acta Biomembr. 1768, 1367–1377. https://doi.org/10.1016/j.bbamem.2006.12.013.

Edwards, K., Almgren, M., 1992. Surfactant-Induced Leakage and Structural Change of Lecithin Vesicles: Effect of Surfactant Headgroup Size. Langmuir 8, 824–832. https://doi.org/10.1021/la00039a016.

Edwards, K., Johnsson, M., Karlsson, G., Silvander, M., 1997. Effect of polyethyleneglycol-phospholipids on aggregate structure in preparations of small unilamellar liposomes. Biophys. J. 73, 258–266. https://doi.org/10.1016/S0006-3495(97)78066-4.

Estes, D.J., Mayer, M., 2005. Electroformation of giant liposomes from spin-coated films of lipids. Colloids Surf. B. 42, 115–123. https://doi.org/10.1016/j.colsurfb.2005.01.016.

Evans, E., Needham, D., 1987. Physical properties of surfactant bilayer membranes: thermal transitions, elasticity, rigidity, cohesion, and colloidal interactions. J. Phys. Chem. 91, 4219–4228. https://doi.org/10.1021/j100300a003.

Evans, E., Rawicz, W., 1990. Entropy-driven tension and bending elasticity in condensed-fluid membranes. Phys. Rev. Lett. 64, 2094–2097. https://doi.org/10.1103/PhysRevLett.64.2094.

Evans, E., Rawicz, W., 1997. Elasticity of “fuzzy” biomembranes. Phys. Rev. Lett. 79, 2379–2382. https://doi.org/10.1103/PhysRevLett.79.2379.

Evans, E., Heinrich, V., Ludwig, F., Rawicz, W., 2003. Dynamic tension spectroscopy and strength of biomembranes. Biophys. J. 85, 2342–2350. https://doi.org/10.1016/S0006-3495(03)74658-X.

Gabizon, A., Papahadjopoulos, D., 1988. Liposome formulations with prolonged circulation time in blood and enhanced uptake by tumors. Proc. Natl. Acad. Sci. 85, 6949–6953. https://doi.org/10.1073/pnas.85.18.6949.

Gabizon, A., Price, D.C., Huberty, J., Bresalier, R.S., Papahadjopoulos, D., 1990. Effect of liposome composition and other factors on the targeting of liposomes to experimental tumors: biodistribution and imaging studies. Cancer Res. 50, 6371–6378.

Gabizon, A., Goren, D., Horowitz, A.T., Tzemach, D., Lossos, A., Siegal, T., 1997. Long-circulating liposomes for drug delivery in cancer therapy: A review of biodistribution studies in tumor-bearing animals. Adv. Drug Deliv. Rev. 24, 337–344. https://doi.org/10.1016/S0169-409X(96)00476-0.

Garbuzenko, O., Barenholz, Y., Priev, A., 2005. Effect of grafted PEG on liposome size and on compressibility and packing of lipid bilayer. Chem. Phys. Lipids 135, 117–129. https://doi.org/10.1016/j.chemphyslip.2005.02.003.

Hashizaki, K., Taguchi, H., Itoh, C., Sakai, H., Abe, M., Saito, Y., Ogawa, N., 2005. Effects of Poly(ethylene glycol) (PEG) Concentration on the Permeability of PEG-Grafted Liposomes. Chem. Pharm. Bull. 53, 27–31. https://doi.org/10.1248/cpb.53.27.

Hossann, M., Kneidl, B., Peller, M., Lindner, L., Winter, G., 2014. Thermosensitive liposomal drug delivery systems: state of the art review. Int. J. Nanomed. 9, 4387–4398. https://doi.org/10.2147/IJN.S49297.

Hristova, K., Needham, D., 1994. The Influence of polymer-grafted lipids on the physical properties of lipid bilayers: a theoretical study. J. Colloid Interface Sci. 168, 302–314. https://doi.org/10.1006/jcis.1994.1424.

Johnsson, M., Hansson, P., Edwards, K., 2001. Spherical micelles and other self-assembled structures in dilute aqueous mixtures of poly(ethylene glycol) lipids. J. Phys. Chem. B 105, 8420–8430. https://doi.org/10.1021/jp011088l.

Karatekin, E., Sandre, O., Guitouni, H., Borghi, N., Puech, P.-H., Brochard-Wyart, F., 2003. Cascades of transient pores in giant vesicles: line tension and transport. Biophys. J. 84, 1734–1749. https://doi.org/10.1016/S0006-3495(03)74981-9.

Klibanov, A.L., Maruyama, K., Torchilin, V.P., Huang, L., 1990. Phospholipids grafted with PEG, known as (PEGylated liposomes) are of major significance for in vivo drug delivery systems. FEBS Lett. 268, 235–237. https://doi.org/10.1016/0014-5793(90)81016-H.

Lasic, D.D., 1997. Recent developments in medical applications of liposomes: Sterically stabilized liposomes in cancer therapy and gene delivery in vivo. J. Control. Release 48, 203–222. https://doi.org/10.1016/S0168-3659(97)00045-X.

Lasic, D.D., 1998. Novel applications of liposomes. Trends Biotechnol. 16, 307–321. https://doi.org/10.1016/S0167-7799(98)01220-7.

Lasic, D.D., Needham, D., 1995. The “Stealth” liposome: a prototypical biomaterial. Chem. Rev. 95, 2601–2628. https://doi.org/10.1021/cr00040a001.

Ly, H.V., Longo, M.L., 2004. The influence of short-chain alcohols on interfacial tension, mechanical properties, area/molecule, and permeability of fluid lipid bilayers. Biophys. J. 87, 1013–1033. https://doi.org/10.1529/biophysj.103.034280.

Marsh, D., 1996. Lateral pressure in membranes. Biochim. Biophys. Acta Biomembr. 1286, 183–223. https://doi.org/10.1016/S0304-4157(96)00009-3.

Marsh, D., 2001. Elastic constants of polymer-grafted lipid membranes. Biophys. J. 81, 2154–2162. https://doi.org/10.1016/S0006-3495(01)75863-8.

Marsh, D., Bartucci, R., Sportelli, L., 2003. Lipid membranes with grafted polymers: physicochemical aspects. Biochim. Biophys. Acta 1615, 33–59. https://doi.org/10.1016/S0005-2736(03)00197-4.

Maruyama, K., Yuda, T., Okamoto, A., Kojima, S., Suginaka, A., Iwatsuru, M., 1992. Prolonged circulation time in vivo of large unilamellar liposomes composed of distearoyl phosphatidylcholine and cholesterol containing amphipathic poly(ethylene glycol). Biochim. Biophys. Acta Lipids Lipid Metab. 1128, 44–49. https://doi.org/10.1016/0005-2760(92)90255-T.

Montesano, G., Bartucci, R., Belsito, S., Marsh, D., Sportelli, L., 2001. Lipid membrane expansion and micelle formation by polymer-grafted lipids: scaling with polymer length studied by spin-label electron spin resonance. Biophys. J. 80, 1372–1383. https://doi.org/10.1016/S0006-3495(01)76110-3.

Needham, D., Rudoll, T.L., 1993. Increased microvascular permeability contributes to preferential accumulation of Stealth[1] liposomes in tumor Tissue[2]. Cancer Res. 53, 3765–3770.

Needham, D., McIntosh, T.J., Lasic, D.D., 1992. Repulsive interactions and mechanical stability of polymer-grafted lipid membranes. Biochim. Biophys. Acta Biomembr. 1108, 40–48. https://doi.org/10.1016/0005-2736(92)90112-Y.

Nicholas, A.R., Scott, M.J., Kennedy, N.I., Jones, M.N., 2000. Effect of grafted polyethylene glycol (PEG) on the size, encapsulation efficiency and permeability of vesicles. Biochim. Biophys. Acta Biomembr. 1463, 167–178. https://doi.org/10.1016/S0005-2736(99)00192-3.

Olbrich, K., Rawicz, W., Needham, D., Evans, E., 2000. Water permeability and mechanical strength of polyunsaturated lipid bilayers. Biophys. J. 79, 321–327. https://doi.org/10.1016/S0006-3495(00)76294-1.

Pantusa, M., Bartucci, R., Marsh, D., Sportelli, L., 2003. Shifts in chain-melting transition temperature of liposomal membranes by polymer-grafted lipids. Biochim. Biophys. Acta Biomembr. 1614, 165–170. https://doi.org/10.1016/S0005-2736(03)00171-8.

Parr, M.J., Ansell, S.M., Choi, L.S., Cullis, P.R., 1994. Factors influencing the retention and chemical stability of poly(ethylene glycol)-lipid conjugates incorporated into large unilamellar vesicles. Biochim. Biophys. Acta Biomembr. 1195, 21–30. https://doi.org/10.1016/0005-2736(94)90004-3.

Pasut, G., Veronese, F.M., 2012. State of the art in PEGylation: The great versatility achieved after forty years of research. J. Control. Release 161, 461–472. https://doi.org/10.1016/j.jconrel.2011.10.037.

Patil, Y.P., Kumbhalkar, M.D., Jadhav, S., 2012. Extrusion of electroformed giant unilamellar vesicles through track-etched membranes. Chem. Phys. Lipids 165, 475–481. https://doi.org/10.1016/j.chemphyslip.2011.11.013.

Portet, T., Dimova, R., 2010. A new method for measuring edge tensions and stability of lipid bilayers: effect of membrane composition. Biophys. J. 99, 3264–3273. https://doi.org/10.1016/j.bpj.2010.09.032.

Rawicz, W., Olbrich, K.C., McIntosh, T., Needham, D., Evans, E.A., 2000. Effect of chain length and unsaturation on elasticity of lipid bilayers. Biophys. J. 79, 328–339. https://doi.org/10.1016/S0006-3495(00)76295-3.

Sandstrom, M.C., Johansson, E., Edwards, K., 2007. Structure of mixed micelles formed in PEG-Lipid/Lipid dispersions. Langmuir 23, 4192–4198. https://doi.org/10.1021/la063501s.

Sriwongsitanont, S., Ueno, M., 2002. Physicochemical properties of PEG-Grafted liposomes. Chem. Pharm. Bull. 50https://doi.org/10.1248/cpb.50.1238. 1238–1238.

Tabarin, T., Martin, A., Forster, R.J., Keyes, T.E., 2012. Poly-ethylene glycol induced super-diffusivity in lipid bilayer membranes. Soft Matter 8, 8743–8751. https://doi.org/10.1039/c2sm25742d.

Woodle, M.C., 1995. Sterically stabilized liposomes therapeutics. Adv. Drug Deliv. Rev. 16, 249–265. https://doi.org/10.1016/0169-409X(95)00028-6.

Woodle, M.C., Newman, M.S., Cohen, J.A., 1994. Sterically Stabilized Liposomes: Physical and Biological Properties. J. Drug Target. 2, 397–403. https://doi.org/10.3109/10611869408996815.